International Journal of Fluid Machinery and Systems
Vol. 4, No. 1, January-March 2011

DOI: 10.5293/IJFMS.2011.4.1.057
ISSN (Online): 1882-9554

Review Paper (Invited)

A Suggested Mechanism of Significant Stall Suppression Effects by Air Separator Devices in Axial Flow Fans

Nobuyuki Yamaguchi

Department of Mechanical Engineering, Meisei University
2-1-1, Hodokubo, Hino-shi, Tokyo, 191-8506, Japan, yamagucn@me.meisei-u.ac.jp

Abstract

Radial-vaned air separators show a strong stall suppression effect in an axial flow fans. From a survey of existing literature on the effects and the author's data, a possible mechanism for the significant effects has been proposed here. The stall suppression is suggested to have been achieved by a combination of the following several effects; (1) suction of blade and casing boundary layers and elimination of embryos of stall, (2) separation and straightening of reversed swirling flow from the main flow, (3) induction of the fan main flow toward the casing wall and enhancement of the outward inclination of meridional streamlines across the rotor blade row, thus keeping the Euler head increase in the decrease in fan flow rate, and (4) reinforcement of axi-symmetric structure of the main flow. These phenomena have been induced and enhanced by a stable vortex-ring encasing the blade tips and the air separator. These integrated effects appear to have caused the great stall suppression effect that would have been impossible by other types of stall prevention devices. Thus the author would like to name the device "tip-vortex-ring assisted stall suppression device".

Keywords: Axial Flow Fan, Stall Suppression, Air Separator, Vortex Ring, Internal Flow

1. Introduction

A variety of casing treatments (abbreviated C.T. hereafter) have currently been being used practically in axial flow fans and compressor stages for stall suppression purpose. Improvement effects by C.T.s in stalling flow rates have been up to from 20 % to 40% at best, depending on the C.T. types and the design parameters and working conditions of the applied fans (Takata, H. [1] and Yamaguchi, N. [2]). The improvement index is defined as a percentage decrease in the stalling flow rate compared with the stalling one for the solid-wall condition (abbreviated S.W. hereafter). On the other hand, air separator devices (abbreviated A.S. hereafter) could show significantly higher effects, showing nearly 100% improvement in flow rate at best, i.e., nearly no stalling up to shut-off condition for lightly loaded fans. The achievements could reasonably be influenced by various conditions of the fans and the devices (for example, Miyake, Y., *et al*. [3], and Yamaguchi, N. *et al*. [4]). Even for highly loaded fans and compressor stages, the improvements could be above 50% (Yamaguchi, N. [6, 7]).

Why could the A.S. effects be so large?

Even if the most uniform inflow field, i.e., the cleanest working environment such as in a two-dimensional flow, could have been established for a blade cascade, the blade or the cascade would never fail to stall beyond some critical angle of attack in the course of decreasing flow rate. Stalling in the C.T. improved conditions is considered to be typical of such situations. An example of flow behaviors in the C.T. situation is described in APPENDIX of this review.

With the simple question in mind, the author has conducted several experiments about the A.S. effects. As a result, a reasonable mechanism for the significant A.S. effects has become apparent within the author's understanding. This paper describes about the concept, which could expectedly contribute to future improvements in stall suppressions in many fluid machinery.

First of all, the mechanism of the A.S. effects appears to be understood very qualitatively as below. Figure 1 shows a schematic view of Ivanov type A.S., which is the prototype of the presently used A.S.devices. Low energy fluid accumulated around the casing wall such as secondary flows and boundary layers on the casing and blades surfaces would tend to be discharged into the inlet slit ① of the device embedded in the casing wall facing the rotor tips, which would make the blade working environment cleaner. With a decrease in the fan flow, embryos of stall, such as small zones of flow reversal and incipient rotating stalls, begin to appear; they tend to have swirls larger than the ambient flow. In the S.W. condition, the flow could interfere directly with the upstream main inflow, tending to force the main flow to become turbulent and unstable. The A.S. device, if equipped, separates and takes in the swirling reversed flows, straighten them into axial one through the rectifying vanes ③ and

Received January 4 2011; accepted for publication January 5 2011: Review conducted by Prof. Kwang-Yong Kim (Paper number R11001K)
Corresponding author: Nobuyuki Yamaguchi, Professor, yamagucn@me.meisei-u.ac.jp

then forces them join smoothly to the main flow through the A.S. exit slit ④, thus stabilizing the flow. The name "air separator" comes from the action.

To be sure, the explanation could be convinced as far as the initial stage of the A.S. action is concerned. However, could it suggest the A.S. effects and mechanisms wholly? This is the main subject of consideration in this paper.

The A.S. device does not have special removal ability. The embryos of stalls, which tend to have larger swirls and therefore greater centrifugal forces than those in the surrounding main flow, could easily enter the A.S. inlet slit ① and inlet pocket ② spontaneously, i.e., by itself. The stronger the degree of the stall, the stronger the action of the separation and discharge becomes. It suggests that the action is a kind of passive stall suppression.

The author would like to think about the phenomena achieved by A.S. devices on the basis of experimental results on the following three points. Although they are separate pieces of rather circumstantial evidence, they could serve totally to construct a reasonable working model of the A.S. action.

(1) Global tendency in changes in stalling points from S.W. conditions to corresponding respective A.S. ones (Section 2).

(2) Influence of A.S. path configurations on the stall suppression effects (Section 3).

(3) Changes in the internal flow patterns achieved in the A.S. conditions compared with S.W. ones (Section 4).

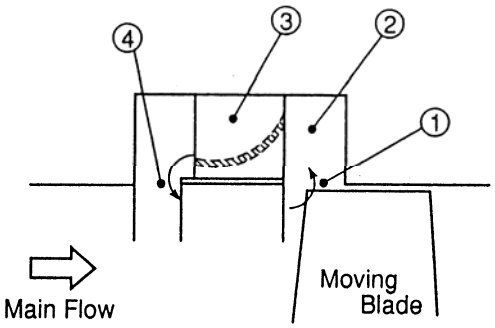

Fig. 1 Structure and flow of an air separator of Ivanov type (axial vane type)

2. Global Tendency in Stall Improvements by Air Separator Devices

Figure 2 shows a rough tendency of improvements of A.S. stalling points from the original S.W. ones surveyed from results of concerned experimental studies on the A.S. effects (Appendix of Yamaguchi, N., *et al*. [4, 5]), which are unfortunately very few in number compared with those on C.T. studies. It plots pressure coefficients vs. flow coefficients both at stalling points related with each other in the S.W. conditions and the A.S. ones. All fans are of axial inlet type bladings. Fan flow coefficients and pressure coefficients at stalling points in A.S. improved conditions and the original S.W. conditions are plotted in a linked fashion in Fig. 2(a) and (b). The coefficients are normalized by rotor tip speeds u_t as follows;

Flow coefficient: $$\phi_t = Q/(Au_t) \tag{1}$$

Total-to-total pressure coefficient: $$\psi_{tT-T} = \Delta p_{T-T}/\left(\rho u_t{}^2/2\right) \tag{2}$$

Total-to-static pressure coefficient: $$\psi_{tT-S} = \Delta p_{T-S}/\left(\rho u_t{}^2/2\right) \tag{3}$$

Here, Q: fan flow rate (m^3/s), A: fan annulus area (m^2), u_t: tip speed of the fan rotor (m/s), $\Delta p_{T\text{-}T}$: fan total-to-total pressure rise (Pa), $\Delta p_{T\text{-}S}$: fan total-to-static pressure rise (Pa), and ρ : density of the flow (kg/m^3). The total-to-static pressure coefficient used here is approximated by the following equation:

Approximate total-to-static pressure coefficient: $$\psi_{tT-S} \approx \psi_{tT-T} - \phi_t{}^2 \tag{4}$$

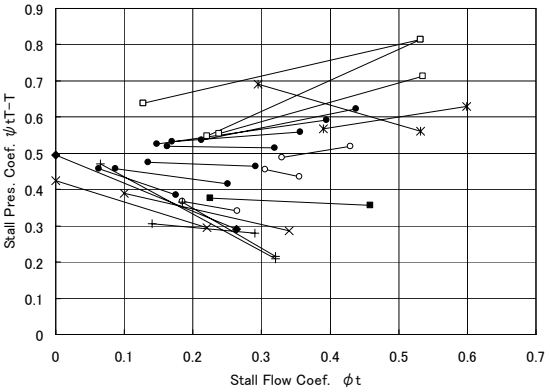

(a) Improvements by A.S. in fan stalling points in terms of total-to-total pressure coefficients

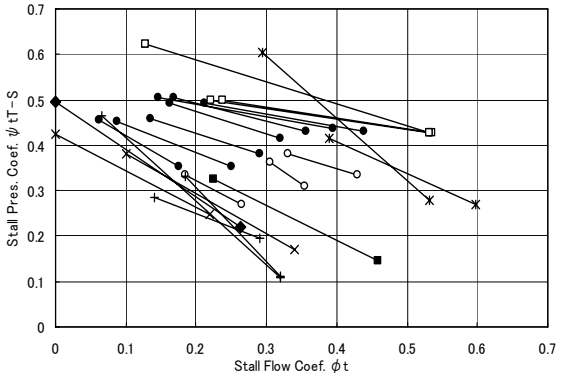

(b) Improvements by A.S. in fan stalling points in terms of total-to-static pressure coefficients

Fig. 2 Global tendency of improvements in stalling points by air separators (including data both for axial-vane type and for radial-vane type)**.** (Yamaguchi, N., *et al.* [4, 5])

Figure 2 contains data for both types of air separators, i.e., Ivanov type having axial vanes (shown in Fig. 1) and radial vane type. An example of the latter is shown in Figs. 6 and 7, and Type IV in Fig. 4, devised by the author but having the same principle as the former. Symbols show the data sources, whose details should be referred to the original report (Yamaguchi, N., *et al*. [4, 5]).

Stalling situations improved by the A.S. devices are shown in Fig. 2(a) in terms of total-to-total pressure coefficients vs. flow coefficients. Each line segment shows its stalling point in the S.W. condition at the right endpoint and its corresponding one improved by an A.S. device at the left endpoint. The connecting straight line neglects the detailed intermediate behavior. Typical examples of the actual behaviors for a highly loaded fan and a lightly loaded fan are seen respectively in Figs. 5 and 8 later. In both examples the behaviors from the S.W. stalling to the A.S. one are seen to be expressed nearly by straight lines.

In Fig.2, lengths of the line segments mean the effectiveness of improvements by the A.S. devices. Generally, a very large improvement in stalling flow by the A.S. devices is noticed. In addition to that, as a very rough trend in Fig. 2(a), the improvements appear to head toward a shut-off pressure coefficient of around 0.5 at zero flow coefficient in spite of the widely scattered S.W. stall points, which reflect a variety of fan design conditions.

Stalling improvements with respect to total-to-static pressure coefficients are shown in Fig. 2(b). All the total-to-static pressure coefficients show negative-slope improvements against flow coefficients, heading toward shut-off pressure coefficient of around 0.5. From another point of view, the attainable maximum total-to-static pressure coefficients appear to lie around 0.5(or 0.4-0.6) at present. Whether it is a limitation of the A.S. capability or a result of insufficient optimization between the fan and the A.S. device is unknown at present.

It should be emphasized that these observations suggest that there exist some common features in the behavior of A.S. improvement process expressed in terms of the rotor-tip normalized quantities. It suggests further that the A.S. improvements could have been caused in general by some common flow structure dominant in the fan tip region or by some common mechanism resulted from them. The cause or the reason of the shut-off pressure coefficient of around 0.5 in the A.S. improved condition is unknown at present, but it also might be related closely with the common mechanism.

There exist of course some data scatter showing deviations from the average tendency and data of insufficient improvements in Fig. 2(a) and (b). It is supposed that they have possibly been influenced by respective designs, geometrical parameters such as hub-to-tip ratio, insufficient optimization between fans and A.S. devices, etc. Highly-loaded fans tend to show relatively less improvements compared with those of lightly-loaded fans. The tendency suggests a need for more studies in the highly-loaded stages for future extended applications to high-pressure axial flow compressor stages in gas turbines, jet engines, industrial compressors, etc.

It is noteworthy here that highly-loaded fans having high S.W. stalling pressure coefficients appear stable yet in a part of positive-slope region of total-to-total characteristics in the A.S. improved conditions in Fig. 2(a) and in Fig. 5 shown later. In other words, such fans tend to stall at some location very deep in the positive-slope region in the A.S. improved total-to-total characteristics. However, the situations are in the negative-slope region in the total-to-static characteristics in Fig. 2(b). It is understood that the fans are stable in the negative-slope region of the total-to-static characteristics, even if they are in the positive-slope region of the total-to-total characteristics.

More exactly, stalling behaviors of total-to-static characteristics curves in the A.S. conditions, converted by Eq. (4) from total-to-total data such as ones in Fig.5, are reducing its negative-slope to near-zero value toward the A.S. stalling points, in a curved fashion different from the straight-line fashion drawn simply in Fig. 2(b). Accordingly, as pointed out generally by Dunham [8], fans including A.S. improved highly-loaded fans should be considered to stall at points of local total-to-static slope of zero in spite of the possible positive slopes in the total-to-total characteristics. Thus it is pertinent to add here that the stalling criterion should be based on the total-to-static basis:

$$\frac{d\Delta p_{T-S}}{dQ} = 0 \tag{5}$$

or

$$\frac{d\psi_{tT-S}}{d\phi_t} = 0 \tag{5a}$$

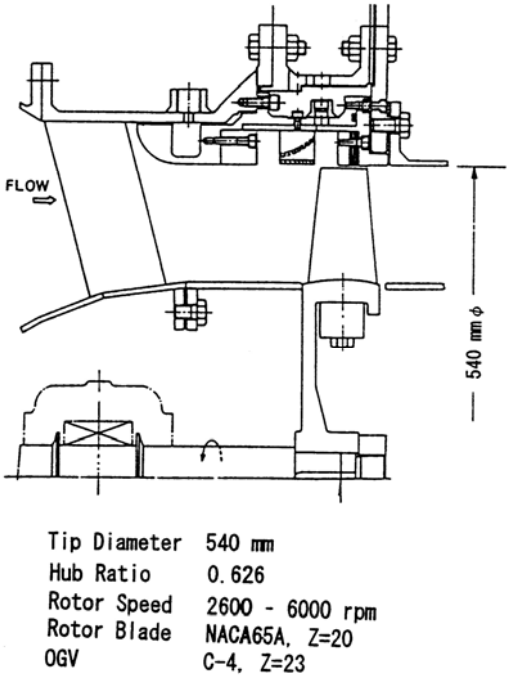

Fig. 3 An experimental fan for study of air separator effects with pressure ratio of around 1.1 at 6000 rpm (Yamaguchi, N., *et al.* [9])

3. Flow Path Configurations of Air Separators and Stall Improvements

Next, let us examine the effects of A.S. flow path configurations on the stall suppression. Yamaguchi, N., *et al.* [9] surveyed such effects experimentally. Figure 3 shows an experimental fan applied with an A.S. device, having relatively high load with pressure ratio of about 1.1 at 6000 rpm. Figure 4 shows A.S. devices for tests, three of which are of Ivanov type having axial straightening vanes (Types I, II, and III) and one is of radial vane type (Type IV) devised by the author.

Total-to-total pressure rise performances of the fan equipped with these A.S. devices are shown in Fig. 5. The tests results obtained at several rpms have been converted to 6000 rpm conditions according to the fan law, which states that fan pressure and flow rate are proportional to its rpm and rpm squared, respectively. The S.W. performance at 6000rpm is shown with solid curves in respective figures. Types I and III are respectively an ordinary Ivanov type with axial vanes and a somewhat improved one with rounded corners of the flow path. The A.S. improvements are large for lower tip speeds but less for higher tip speeds. Type III is rather better than Type I preferably because of its smoother flowpath configuration. A.S. Type II has an inlet pocket with a slant wall pushing the incoming flow into the axial straightening vanes. Possibly as the result, as shown in Fig. 5(b), rather better stall suppression effects are attained compared with those of Types I and III particularly at lower tip speeds. Type II and III shows roughly 30% improvements in the stallling flow rate at high speeds of 6000 and 4500 rpms. On the other hand, A.S. Type IV

having radial vanes shows stall improvements of roughly 50%, irrespectively of the tip speeds. From the results, it could be said that in comparison with other types, Type IV is excellent in that stall improvement is both very effective and stable, unaffected by the tip speeds.

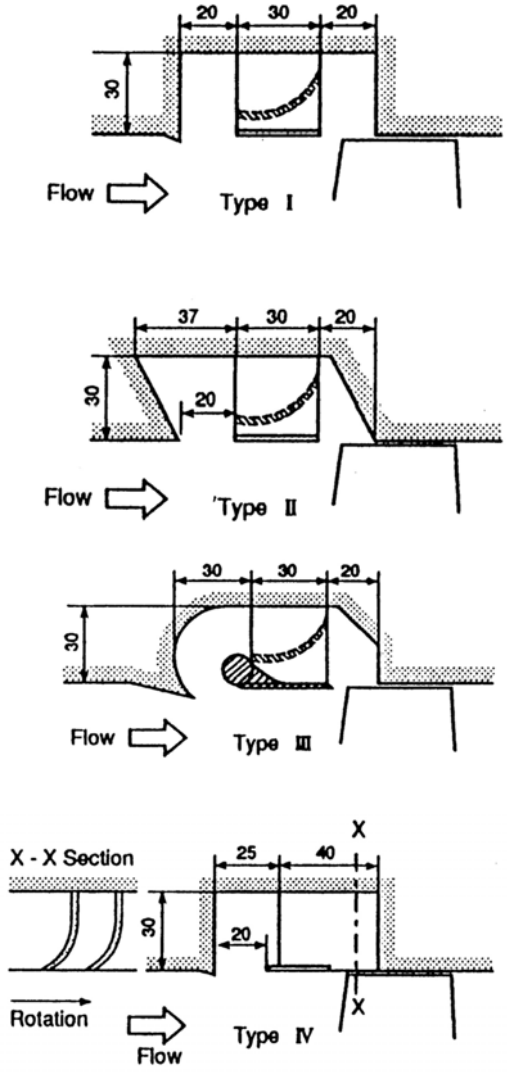

Fig. 4 Four types of air separator devices for the fan shown in Fig. 3 (Yamaguchi, N., *et al.* [9])

These results appear to show an importance of the A.S. flow path configurations in the stall improvement process. No other detailed data are available except the overall performance results in Fig. 5. So, the author cannot help depending on his personal suppositions and feelings, which might be said as follows.

(1) Comparison of the performances resulted by Type IV and Types I-III suggests a rather unfavorable influence of the A.S. inlet pocket (② shown in Fig. 1) provided in the latter three. Flows leaving from the rotor tips would form a strong circumferentially swirling vortex flow in the pocket, which has its apparent center of rotation at the fan axis. However, it could have unfavorable nature of bad circularity, such as moving-around vortex center, imperfect circle shapes, transiently changing shapes, etc. The situation would tend to interfere retroactively with the fan main flow and could generate turbulence and premature instability in high speed conditions, although there remain some extent of stall improvements.

(2) The circumferentially swirling vortex in the pocket could affect another vortex flow, i.e., the recirculation flow in the A.S. path, which is a tip vortex ring shown in Fig. 12. The complicated interaction between the circumferential vortex and the tip vortex

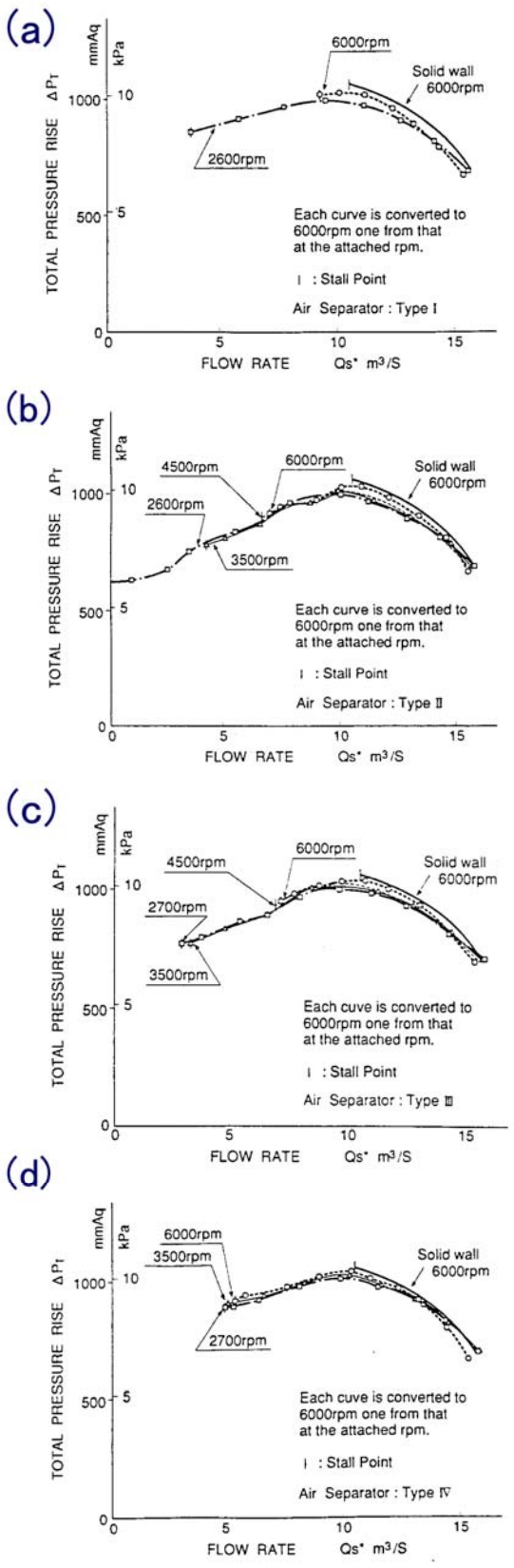

Fig. 5 Stalling Behaviors obtained by respective air separator types; (a) Type I, (b) Type II, (c) Type III, and (d) Type IV shown in Fig. 4 (Yamaguchi, N., *et al.* [9])

ring might result in the difference in the stall improvements. In lower tip speeds, the vortices might be rather favorable and stable, but in higher tip speeds they could tend to become turbulent and destructive.

As seen in the performance of Type II in Fig. 5(b), the situation might be improved somewhat, if the circumferential vortex could be pushed into the axial straightening vanes sooner, which could have contributed to lessening the unfavorable interaction.

(3) On the other hand, A.S. Type IV having radial vanes without an inlet pocket could straighten directly the swirling inflow, forming easily the tip vortex ring. The flow structure around the blade tips and the A.S. device would be stabilized, which is suggested by the fact seen in Fig. 5(d) that the stall improvements are stable irrespective of the fan speed over the whole speed range tested.

From the above observation and supposition based on the results in Fig. 5, it is supposed that the tip vortex ring through the A.S. flow passage could be a key player in the stall stabilization process. Therefore the strength and the stability of structure of the vortex ring could have a very important significance in the process.

In addition to the above, temperature rises in the machine wall around the A.S. devices were sensed on the site of the experiments, which suggests rotor works given repeatedly to the A.S. flow circulating in the tip vortex ring. It is a kind of proof about the presence of a tip vortex. However, it would possibly present a problem in applying A.S. devices to high-load fans and high-speed compressor stages from an aspect of mechanical safety.

As seen in Fig. 5, the A.S. improved part of the fan characteristics has positive-slopes in the total-to-total pressure characteristics. Namely, the A.S. improved fan stallings have occurred deep into the positive-slope region. The fan was safely operated in the A.S. condition until the occurrence of stall. The stalling points (or surge points) were clearly distinguished even in the A.S. improved conditions by sudden bangs in the machine noises and vibrations in the measurements. Slopes of total-to-static pressure characteristics curves converted by Eq. (4) from the total-to-total ones tend to near-zero value near the A.S. stalling points, although in the simplified tendency in Fig. 2(b) the stallings seem to occur in the negative slope region. Therefore, the stallings should be considered to have occurred according to Eq. 5 on the total-to-static base. From a point of local instability, i.e., occurrence of rotating stalls, the judgment is considered to be valid. However, from a point of global instability, i.e., system instability or surging of a fan coupled with a system of ductings, it might require a more detailed consideration.

4. Internal Flows Affected by A.S. Devices

Then, what changes occur in the internal flows in fans equipped with an A.S. device? Yamaguchi, N., et al. [10] surveyed the internal flow patterns in a lightly-loaded fan with and without an A.S. device. The experimental fan and the A.S. device are shown in Fig. 6 and 7, respectively. Internal flows were measured at flow coefficients numbered in Fig. 8, where the ordinate is total-to-total pressure coefficient between upstream and downstream of the rotor blade row, normalized by the rotor tip-speed dynamic pressure. The A.S. device of radial vane type has achieved a nearly stall-free characteristics shown in fig.8.

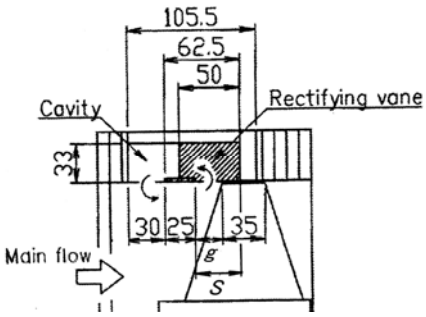

Fig. 6 An experimental fan for study of the A.S. effects on the internal flows related with the contents in Section 4. Casing diameter:394 mm, rotor tip diameter: 390 mm, hub diameter: 194 mm, speed: 2600 rpm. (Yamaguchi, N., *et al.* [10])

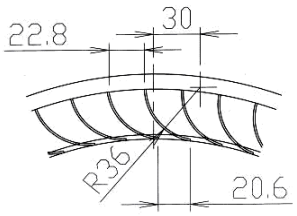

Fig. 7 Configuration of the radial straightening vanes employed in the fan shown in Fig. 6 (Yamaguchi, N., *et al.* [10])

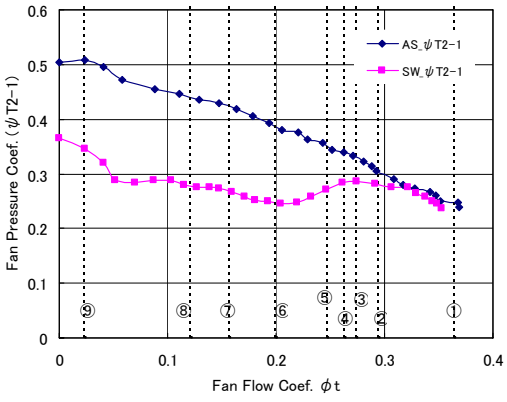

Fig. 8 Fan performance characteristics obtained for the solid wall condition (S.W.) and the air separator condition (A.S.). Encircled numerical figures show conditions of internal surveys (Ya maguchi, N., *et al.* [10])

Figure 9 (a) and (b) show radial distributions of axial velocities and swirl velocities normalized by the rotor tip speed, V_{a2}/u_t and V_{u2}/u_t respectively, downstream of the rotor for the S.W. condition. The abscissa is radial location normalized by the rotor tip radius (r/r_t). Figure 10 (a) and (b) show distributions of the same kind for the A.S. condition. Here the symbols are ; r : radial location, r_t : radius of the rotor tip, V_{a2} : axial velocity downstream of the rotor, and V_{u2} : swirl velocity downstream of the rotor. Comparison of these velocity distributions has shown marked differences in the flow behaviors between the A.S. and S.W. conditions. In the A.S. condition, for reducing fan flow rate, the axial velocity distributions (Fig. 10(a)) tend to change its pattern in the radial direction, increasing toward the casing wall and decreasing toward the hub. This change means meridional streamlines forced to incline toward the casing within the rotor with the reduction in the fan flow rate. In contrast, in the S.W. condition, the velocity distributions (Fig. 9(a)) are ordinary ones only with its average level changing, suggesting nearly parallel meridional

streamlines. The meridional streamlines estimated from the axial velocity distributions are shown in Fig. 11 for the S.W. condition (a) and the A.S. condition (b). Figures for SW_1 and AS_1, SW_4 and AS_4, and SW_6 and AS_6, and AS_8 are corresponding, respectively, to the maximum flow condition ①, nearly stalling condition of S.W. and equivalent flow for A.S.④, and after stalled condition of S.W. and equivalent flow for A.S.⑥, and the A.S. condition at the flow rate corresponding to that in deep stall condition ⑧ of S.W., shown in the overall characteristics in Fig.8. Since these streamlines are connected with straight lines between corresponding points upstream and downstream rather far away from the rotor blading, the real difference between both streamlines could be larger. In fact, experimental data suggested steeper streamlines across the rotor blading (Yamaguchi, N., *et al*. [9]).

The enhanced outward inclination of the meridional streamlines would help increase the rotor pressure rise according to the Euler head equation. The swirl velocities continue to increase radially outward as seen in Fig. 10(b), compared with those in the S.W. condition in Fig. 10(a). Thus the negative-slope of pressure vs. flow characteristics could be maintained down to very small flow rate in the A.S. conditions.

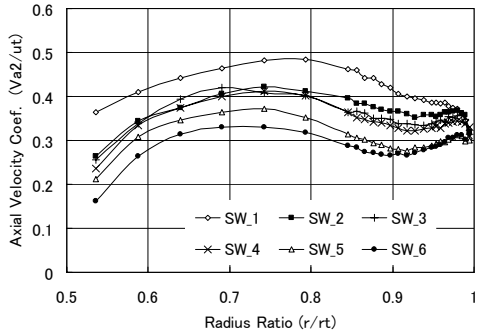

(a) Axial velocity component

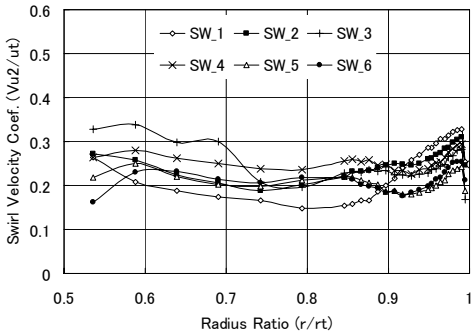

(b) Swirl velocity component

Fig. 9 Radial distributions of flow velocities downstream of the rotor blades for S.W. conditions (Yamaguchi, N., et al. [10])

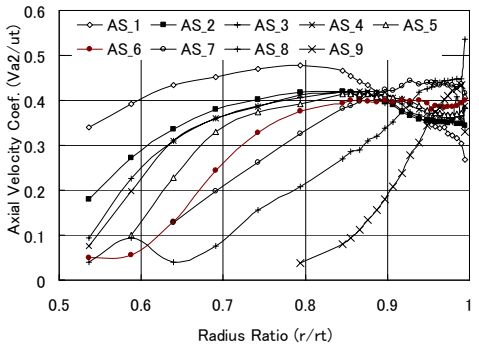

(a) Axial velocity component

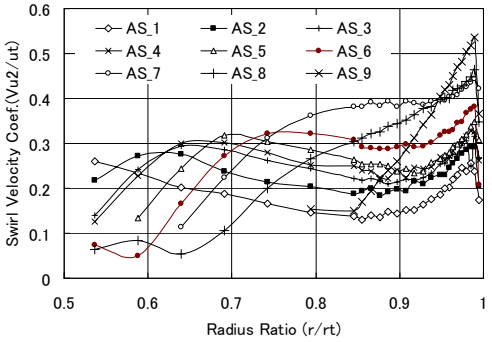

(b) Swirl velocity component

Fig. 10 Radial distributions of flow velocities downstream of the rotor blades fo A.S. condition (Yama guchi, N., et al. [10])

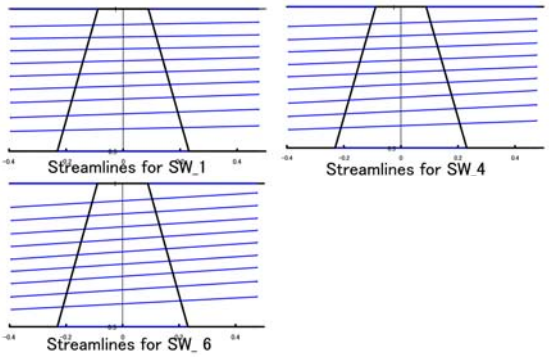

(a) Streamlines for the S.W. condition

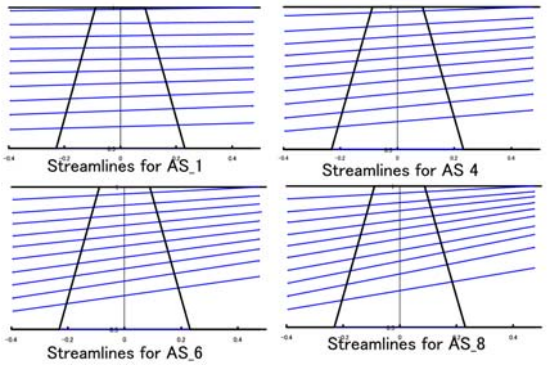

(b) Streamlines for the A.S. condition

Fig. 11 Estimated meridional streamlines across the rotor blade row for the S.W. conditions and the A.S. ones (Yamaguchi, N., *et al*. [10])

These observations lead to the consideration that it is the rotor-tip vortex ring (meridional vortex) through the A.S. passage that reinforces and stabilizes the outward inclination of the meridional streamlines. The vortex ring located around the tip leading edges of the rotor blade rows would tend to attract the flow within the rotor blades toward the casing wall, forcing the streamlines

incline outward. With a decrease in the fan flow, the vortex flow rate increases comparatively, resulting in increased vortex strengths and increased streamline inclinations. Thus the fan pressure rise would increase further.

Furthermore, the increased vortex strength will enhance the axi-symmetry of the flow. The situation will provide stabilization of flow structure and further suppression of stalling tendency. The author supposes that, at the same time, the enhanced axi-symmetry could suppress initiation of rotating stalls that are circumferential instability.

5. Summary on the Mechanism of the Air Separator Devices

Integration of the above-described matters would lead to the following conclusion as to the mechanism of the A.S. effects. For decreasing fan flow rate, the following sequence of phenomena will appear in the A.S. applied conditions, resulting in the excellent unstalling capability of the fans.

(1) Improvement of blade working environment caused by discharge of blade tip low-energy flow
(2) Prevention of generation of turbulence and instability in the main flow by separation and straightening of embryos of stalls such as small reversal of flow, incipient rotating stalls, low-energy stagnant flows around rotor blade tips
(3) Induction of flow around the rotor blade tips toward the casing wall by discharge of the flow
(4) Resulting generation of outward-inclined meridional streamlines across the rotor
(5) Increase in fan pressure and maintained negative-slope characteristics resulted from the Euler pressure along the inclined meridional streamlines
(6) Appearance of stable tip vortex ring encasing the blade tips owing to relative increase in the circulating flow through the A.S. passage
(7) Enhanced axi-symmetry of the rotor internal flow structure by the presence of the stable tip vortex ring
(8) Further enhanced streamline inclinations and continued negative-slope characteristics

In summary, the actions of “air separator” mentioned (1) and (2) above work effectively at the initial stage as well as those in casing treatment situations. In the following stage, outward inclined meridional streamlines are created by the tip vortex ring and the resulting Euler pressure maintains the negative-slope characteristics. Finally the strong tip vortex ring dominates the flow field, enhancing the axi-symmetry of the flow structure. Thus a great stall suppression effects could be achieved. A schematic model of the flow field is shown in Fig. 12.

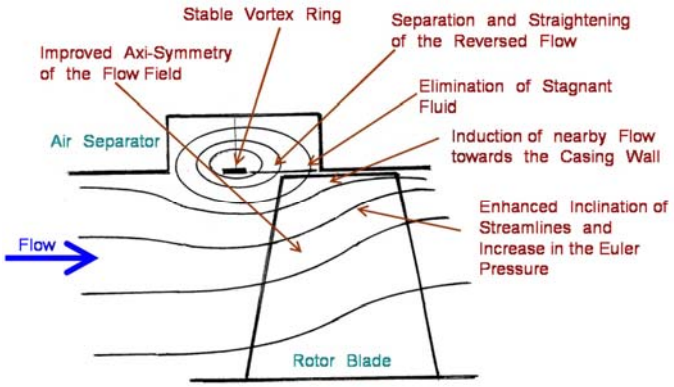

Fig. 12 Qualitative sketch showing the flow field and the effects in a radial-vaned air-separator applied fan

Thus, it is understood that the flow structure dominated by the vortex ring encasing the blade tips would bring about the global tendency observed in Fig. 2, that is, tip-normalized stalling-pressure coefficients tend to a value of around 0.5 at the shut-off condition. Consequently the A.S. passage configurations easier to realize stable and strong tip vortex rings would be more effective in stall suppression. From the line of thinking, the author would like to suggest naming the A.S. device ”tip-vortex-ring enhanced (or assisted) stall stabilizing device”.

In relation to the above, axial flow fans and pumps designed for very low flow-coefficients tend to have no positive-slope characteristics (Ikui, T., et al. [11]), where tip vortex ring situations similar to the above-stated one are considered to occur spontaneously. In the sense, A.S. devices could be said to bridge the S.W. stalling condition to such spontaneous stable vortex structures through artificial vortex rings.

6. Concluding Remarks

The mechanism of the excellent stall suppression effects achieved by air separator devices is suggested on the basis of some experimental results, though including several suppositions. The mechanism presented here will help researches and developments where more improvements are desired, for example, in highly loaded fans and compressor stages.

The air separator devices have many advantages of the significant stall suppression effects and the nature of passive stall control, and possible easiness in manufacture and application if the structures are devised. The author expects that they will be put to practical use more generally in future.

APPENDIX

Velocity Distributions near Stalling Conditions Improved by a Casing Treatment

An additional example of internal flows in the neighborhood of stalling in the condition improved by a casing treatment (C.T. hereafter) is described for reference (Yamaguchi, N., *et al.* [11]).

Figure A-1 shows an experimental three-stage axial flow compressor. The first-stage has a tip diameter 500 mm and hub-to-tip radius ratio 0.67. The measurements were conducted at 2000 rpm although the design speed was 12000 rpm. All the stages were equipped with a C.T. insert of the axial slot type shown in Fig. A-2.

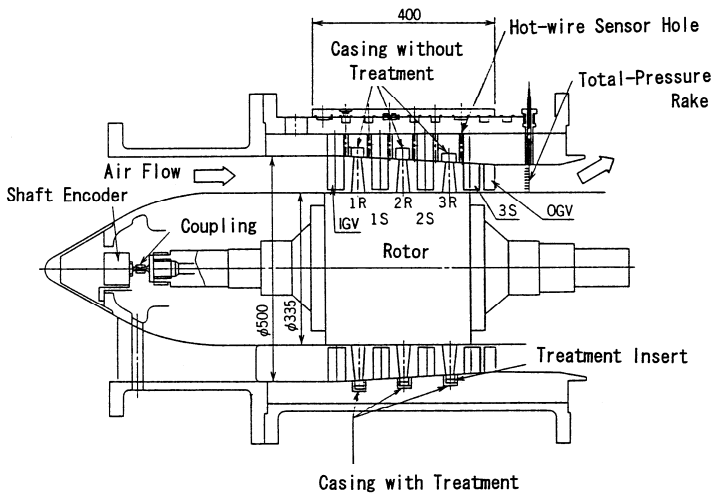

Fig. A-1 Experimental low-speed compressor for study of casing treatment effects (Yamaguchi, N. and Higaki, T. [11])

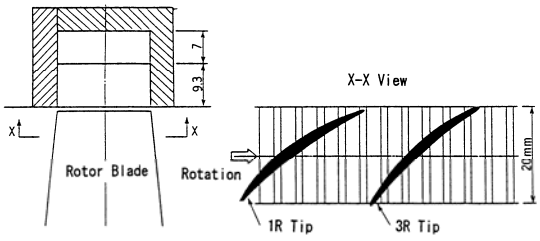

Fig. A-2 Casing treatment insert employed in the study in Fig. A-1 (Yamaguchi, N. and Higaki, T. [11])

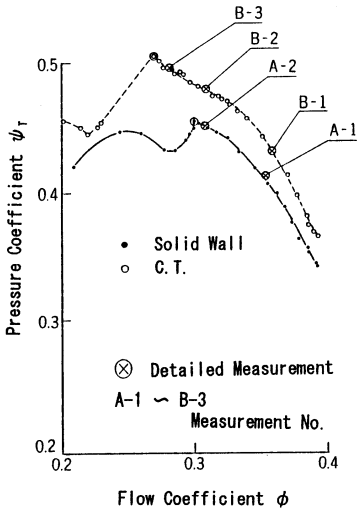

Fig. A-3 Characteristic curves of the first stage for the S.W. condition and the C.T. condition (Yamaguchi, N. and Higaki, T. [11])

The characteristics of the first stage is shown in Fig. A-3. The compressor stalled at the first stage because of the very low speed operation. Stalling flow improvement is roughly 10%. At some typical points shown in Fig. A-3, the internal flows were surveyed by a hot-wire anemometer system of phase-locked measurements and circumferentially averaging. The results are shown in Fig. A-4 where ϕ is axial flow velocity coefficient (V_a/u_t), λ is swirl velocity coefficient (V_u/u_t), and ρ is radial velocity coefficient (V_r/u_t). The variables are normalized by the rotor tip speed u_t; suffix 2 means the measuring location downstream of the rotor blades. The ordinate is relative radial location.

Figure A-4(a) shows flow distributions downstream of the rotor blade row in the S.W. condition. The axial flow velocity distributions show fairly thick casing boundary layers, in relation with which the swirl velocity distributions show large bulges near the casing wall.

On the other hand, in the internal flows in the C.T. condition shown in Fig. A-4(b), the axial velocity distributions becomes more uniform close to the casing wall, and at the same time, the bulges of the swirl distribution have disappeared. The radial distributions become relatively close to the designed distributions shown with one-dot chain lines.

As understood from a comparison of Fig. A-4(a) and (b), the flow conditions near the casing wall for the C.T. condition have become generally more uniform and cleaner compared with the S.W. one. The situation is similar also for point B-3 near the stall point in the C.T. condition with the axial velocity and the swirl velocity showing only small reduction toward the casing wall. The inverse tendency, i.e., axial and swirl velocity distributions increasing toward the casing wall such as observed in Fig. 10 for the A.S. condition, does not exist for the C.T. improvement.

With respect to the effects of the C.T., it is considered that the air compressed into the C.T. insert from the blade pressure surface region of a passing blade is blown back into the blade suction region immediately after the blade has passed (Takata, H. and Tsukuda, Y. [12]). The blown-back jet sweeps away low–energy flow region and make the blade tip environment cleaner. An example of the resulting flow field is the one shown in Fig. A-4(b). Thus, it is the C.T. effects that make the tip flow field more uniform, where the blades are able to work to its ideal stalling angle of attack.

From the line of thinking, the C.T. action would be difficult to cause outward inclinations of meridional streamlines across the rotor blade row. Therefore the negative-slope characteristics by the Euler pressures along the streamlines would hardly be expected. That is to say, the C.T. action would be difficult to proceed to the next stage、i.e., tip vortex ring assisted stall suppression that has been suggested above for the A.S. effects.

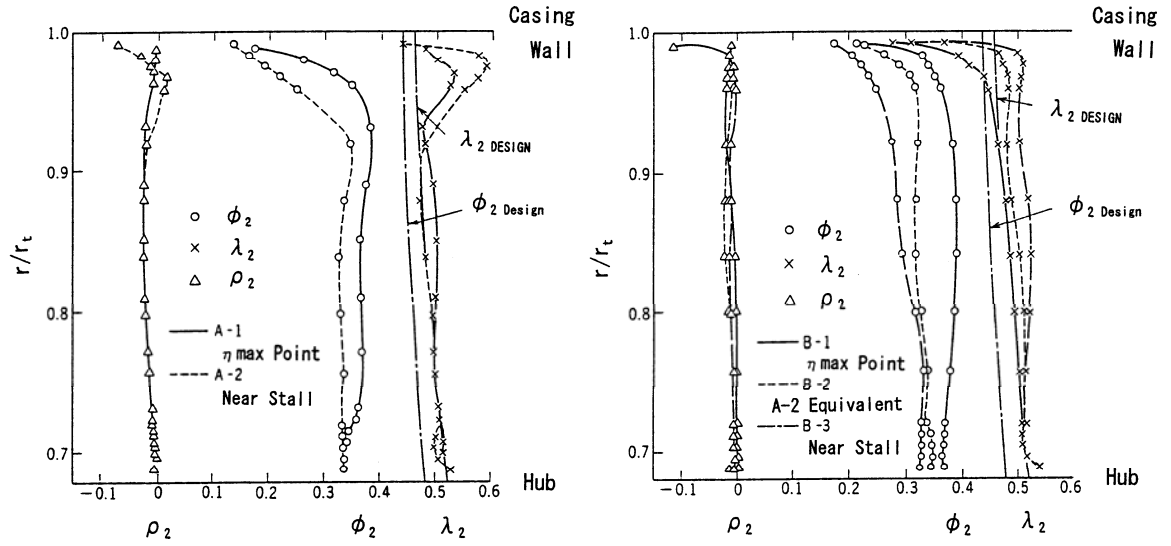

Fig. A-4 Velocity distributions downstream of the first stage rotor for the solid-wall condition and the casing-treated one (Yamaguchi, N. and Higaki, T. [11])

Acknowledgment

The author would like to express his hearty thanks to Professor Yoshinobu TSUJIMOTO, Osaka University, Japan, who has recommennded to submit this paper to IJFMS and has given many valuable advices about the contents. The author would like also to express his thanks to Associated Professor Masayuki OGATA, Meisei University, and many students of Dept. of Mechanical Engineering, Meisei University, and to many engineers at Takasago Research and Development Center, Mitsubishi Heavy Industries, Ltd. who have devoted their efforts to the experimental studies on the effects of air separators and casing treatments, the results of which have been cited in this paper.

Symbols

A	Fan annulus area [m^2]
A.S.	Air separator condition
C.T.	Casing treatment condition
p	Fan pressure [Pa]
p_S	Fan static pressure [Pa]
Q	Fan flow rate [m^3/s]
r	Radial location [m]
r_t	Tip radius of the rotor blades [m]
S.W.	Solid wall condition
u_t	Blade tip circumferential speed [m/s]
Va_2	Axial velocity downstream of the rotor blade row [m/s]
Vu_2	Swirl velocity downstream of the rotor blade row [m/s]
$\Delta p_{T\text{-}S}$	Fan total-to-static pressure rise [Pa]
$\Delta p_{T\text{-}T}$	Fan total-to-total pressure rise [Pa]
ϕ	Axial velocity normalized by rotor blade tip speed (Appendix)
ϕ_t	Flow coefficient normalized by rotor blade tip speed
$\psi_{t\ T\text{-}S}$	Fan total-to-static pressure coefficient normalized by rotor blade tip speed
$\psi_{t\ T\text{-}T}$	Fan total-to-total pressure coefficient normalized by rotor blade tip speed
ρ	Density of the flow [kg/m^3] Radial velocity normalized by rotor blade tip speed (Appendix)
λ	Swirl velocity normalized by rotor blade tip speed (Appendix)
Suffix	
2	Location downstream of the rotor blade row

References

[1] Takata, H., 1991, “Lecture on Stall Control Technologies in Compressors (in Japanese),” 181-th Seminar, Kansai Chapter of Japan Society of Mechanical Engineers, pp. 45-56.
[2] Yamaguchi, N., et al., 1983, “Development of Axial-Type Primary Air Fan for Coal-Fired Boilers-Development of Casing-Treated Adjustable Moving-Blade Axial Fans- (in Japanese),” Mitsubishi Juko Giho (Technical Review of Mitsubishi Heavy Industries, Ltd.), Vol. 20, No. 3 (The content is translated in Technical Review of Mitsubishi Heavy Industries, Ltd., Oct., 1983).
[3] Miyake, Y., et al., 1984, “Aerodynamic Characteristics of Axial Flow Fans Equipped with Air Separators (in Japanese),” Transaction of the Japan Society of Mechanical Engineers (B), Vol. 50, No. 460, pp. 2960-2967.
[4] Yamaguchi, N., Ogata, M., and Kato, Y., 2008, “Improvement of Stalling Characteristics of an Axial Fan by Radial-Vaned Air-Separators (in Japanese),” Transaction of the Japan Society of Mechanical Engineers (B), Vol. 74, No. 746, pp. 2163-2172.
[5] Yamaguchi, N., Ogata, M., and Kato, Y., 2010, “Improvement of Stalling Characteristics of an Axial Fan by Radial-Vaned Air-Separators,” Journal of Turbomachinery, Transaction of the ASME, Vol. 132, No. 2, pp. 021015-1-10.
[6] Yamaguchi, N., Takami, I. and Arimura, H., 1991, “Improvement of Air Separators of Axial Blowers (in Japanese),” Proceedings of 250-th Meeting of Kansai Chapter, the Japan Society of Mechanical Engineers, pp. 176-178.
[7] Yamaguchi, N., et al., 1994, “Development of Mitsubishi General-Purpose Axial Fan (WIDEMAX Fan) (in Japanese),” Mitsubishi Juko Giho (Technical Review of Mitsubishi Heavy Industries, Ltd.), Vol. 31, No. 3, pp. 201-204.
[8] Dunham, J., 1965, "Non-Axisymmetric Flows in Axial Compressors,” Institution of Mechanical Engineers, Mechanical Engineering Science Monograph No. 3, Oct.
[9] Yamaguchi, N., Ogata, M. and Tanaka, S., 2010, “Experimental Study on the Mechanism of Significant Stall Suppression Effects in an Axial Flow Fan Achieve by Air Separator Device (in Japanese),” Transaction of the Japan Society of Mechanical Engineers (B), Vol. 76, No. 771, pp. 1727-1735.
[10] Ikui, T., et al., 1973, “Design Concept and Post-Stall Behaviors of Axial Flow Fans and Blowers (1) (in Japanese),” Researches on Machines, Yokendo Publishing Company, Japan, Vol. 25, No. 10, pp. 1275-1280.
[11] Yamaguchi, N. and Higaki, T., 1984, “Effects of Casing Treatment on Aerodynamic Performance and Internal Flow of Axial Flow Blowers (in Japanese),” Mitsubishi Juko Giho (Technical Review of Mitsubishi Heavy Industries, Ltd.), Vol. 21, No. 3, pp. 40-46.
[12] Takata, H. and Tsukuda, Y., “Stall Margin Improvements by Casing Treatment-Its Mechanism and Effectiveness,” J. Eng. and Power, Trans. ASME, 1977, Vol. 99, No. 1, pp. 121-133.

Nobuyuki Yamaguchi Professor of Dept. of Mechanical Engineering, Faculty of Sciences and Engineering, Meisei University, Tokyo, Japan, (1994-present). Field of activity: aerodynamics of axial flow compressors and fans, fluid mechanics and engineering in industrial equipments and phenomena.
R and D engineer (1965-1994) at Takasago R and D Center, Mitsubishi Heavy Industries, Ltd.. He had been engaged in R and D of axial flow compressors and fans for industrial use and for gas turbines.
BA(1963) , MA (1965) and Dr.Eng. (1978) from Tokyo University